"Science Stays True Here"
Biological and Chemical Research, 55-71 | Science Signpost Publishing

Structural-Parametric Model of Electromagnetoelastic Actuator for Nano- and Micromanipulators of Biological and Chemical Research

S.M. Afonin

Department of Intellectual Technical Systems, National Research University of Electronic Technology (MIET), 124498 Moscow, Russia.

Received: November 02, 2016 / Accepted: December 06, 2016 / Published: March 25, 2017

Abstract: Structural-parametric model, parametric structural schematic diagram, transfer functions of electromagnetoelastic actuator are obtained. Effects of geometric and physical parameters of electromagnetoelastic actuators and external load on its dynamic characteristics are determined. For calculation of control systems with piezoactuators the parametric structural schematic diagram and the transfer functions of piezoactuators are obtained. A generalized parametric structural schematic diagram of the electromagnetoelastic actuator is constructed.

Key words: electromagnetoelastic actuators, piezoactuator, deformation, nano- and micromanipulators, decision wave equations, structural-parametric model, parametric structural schematic diagram, transfer functions

1. Introduction

Electromagnetoelastic actuators for nano- and micromanipulators of biological and chemical research operate on electromagnetoelasticity (piezoelectric, piezomagnetic, electrostriction, and magnetostriction effects). Its application is promising in nanobiology, nanotechnology, microelectronics, power engineering, astronomy for large compound telescopes, antennas satellite telescopes and adaptive optics equipment for precision matching, compensation of temperature and gravitation deformations, and atmospheric turbulence via wave front correction. Piezoactuator - piezomechanical device intended for actuation of mechanisms, systems or management based on the piezoelectric effect, converts electrical signals into mechanical movement and force [1-4].

In the present paper is solving the problem of building the structural parametric model of the

Corresponding author: S.M. Afonin, Department of Intellectual Technical Systems, National Research University of Electronic Technology (MIET), 124498 Moscow, Russia. E-mail: eduems@mail.ru.

electromagnetoelastic actuator in contrast its electrical equivalent circuit [5-7]. By solving the wave equation with allowance methods of mathematical physics for the corresponding equation of electromagnetoelasticity, the boundary conditions on loaded working surfaces of a electromagnetoelastic actuators, and the strains along the coordinate axes, it is possible to construct a structural-parametric model of the actuator. The transfer functions and the parametric structural schematic diagrams of the electromagnetoelastic actuators are obtained from a set of equations describing the corresponding structural-parametric model of the actuator for control systems [8-21].

The piezoactuator of nanometric movements operates based on the inverse piezoeffect, in which the motion is achieved due to deformation of the piezoelement when an external electric voltage is applied to it. Piezoactuators for drives of nano- and micrometric movements provide a movement range from several nanometers to tens of microns, a sensitivity of up to 10 nm/V, a loading capacity of up to 1000 N, the power at the output shaft of up to 100 W, and a ransmission band of up to 1000 Hz. The investigation of static and dynamic characteristics of a piezoactuator is necessary for calculation mechatronic systems of nano- and micrometric movements. At the nano- and microlevels, piezoactuators are used in linear nano- and microdrives and micropumps. Piezoactuators provide high stress and speed of operation and return to the initial state when switched off; they have very low displacements. Piezoactuators are used in the majority of nanomanipulators for scanning tunneling microscopes (STMs), scanning force microscopes (SFMs), and atomic force microscopes (AFMs). Nanorobotic manipulators with nano- and microdisplacements with piezoactuators based are a key component in nano- and microdisplacement precision systems for biological and chemical research [22-30].

2. Structural-Parametric Model and Parametric Structural Schematic Diagram of Electromagnetoelastic Actuator

In the piezoactuator there are six stress components T_1, T_2, T_3, T_4, T_5, T_6, the components T_1 - T_3 are related to extension-compression stresses, T_4 - T_6 to shear stresses.

The matrix state equations [7] connecting the electric and elastic variables for polarized ceramics have the form

$$\mathbf{D} = \mathbf{dT} + \boldsymbol{\varepsilon}^T \mathbf{E}\,, \tag{1}$$

$$\mathbf{S} = \mathbf{s}^E \mathbf{T} + \mathbf{d}^t \mathbf{E}\,. \tag{2}$$

Here, the first equation describes the direct piezoelectric effect, and the second - the inverse piezoelectric

effect; **S** is the column matrix of relative deformations; **T** is the column matrix of mechanical stresses; **E** is the column matrix of electric field strength along the coordinate axes; **D** is the column matrix of electric induction along the coordinate axes; $\mathbf{s}^E$ is the elastic compliance matrix for $E = \text{const}$; and $\mathbf{d}^t$ is the the transposed matrix of the piezoelectric modules.

In polarized ceramics PZT there are five independent components s_{11}^E, s_{12}^E, s_{13}^E, s_{33}^E, s_{55}^E in the elastic compliance matrix, three independent components d_{33}, d_{31}, d_{15} in the transposed matrix of the piezoelectric modules and three independent components $\varepsilon_{11}^{\mathrm{T}}$, $\varepsilon_{22}^{\mathrm{T}}$, $\varepsilon_{33}^{\mathrm{T}}$ in the matrix of dielectric constants.

The equation of electromagnetoelasticity of the actuator [7] has the form

$$S_i = s_{ij}^{E,H,\Theta} T_j + d_{mi}^{H,\Theta} E_m + d_{mi}^{E,\Theta} H_m + \alpha_i^{E,H} \Delta\Theta, \tag{3}$$

where S_i is the relative deformation along the axis *i*, *E* is the electric field strength, *H* is the magnetic field strength, Θ is the temperature, $s_{ij}^{E,H,\Theta}$ is the elastic compliance for $E = \text{const}$, $H = \text{const}$, $\Theta = \text{const}$, T_j is the mechanical stress along the axis *j*, $d_{mi}^{H,\Theta}$ is the piezomodule, i.e., the partial derivative of the relative deformation with respect to the electric field strength for constant magnetic field strength and temperature, i.e., for $H = \text{const}$, $\Theta = \text{const}$, E_m is the electric field strength along the axis m, $d_{mi}^{E,\Theta}$ is the magnetostriction coefficient, H_m is the magnetic field strength along the axis m, $\alpha_i^{E,H}$ is the coefficient of thermal expansion, $\Delta\Theta$ is deviation of the temperature Θ from the value $\Theta = \text{const}$, *i* = 1, 2, … , 6, *j* = 1, 2, … , 6, *m* = 1, 2, 3.

When the electric and magnetic fields act on the electromagnetoelastic actuator separately, we have the respective electromagnetoelasticity equations [7, 9] as the equations of inverse piezoelectric effect:

$S_3 = d_{33}E_3 + s_{33}^E T_3$ for the longitudinal deformation when the electric field along axis 3 causes deformation along axis 3,

$S_1 = d_{31}E_3 + s_{11}^E T_1$ for the transverse deformation when the electric field along axis 3 causes deformation along axis 1,

$S_5 = d_{15}E_1 + s_{55}^E T_5$ for the shift deformation when the electric field along axis 1 causes deformation in the plane perpendicular to this axis,

as the equations of magnetostriction:

$S_3 = d_{33}H_3 + s_{33}^H T_3$ for the longitudinal deformation when the magnetic field along axis 3 causes deformation along axis 3,

$S_1 = d_{31}H_3 + s_{11}^H T_1$ for the transverse deformation when the magnetic field along axis 3 causes deformation along axis 1,

$S_5 = d_{15}H_1 + s_{55}^H T_5$ for the shift deformation when the magnetic field along axis 1 causes deformation in the plane perpendicular to this axis.

Let us consider the longitudinal piezoelectric effect in a piezoelectric actuator shown in Fig. 1, which represents a piezoelectric plate of thickness δ with the electrodes deposited on its faces perpendicular to axis 3, the area of which is equal to S_0. The direction of the polarization axis *P*, i.e., the direction along which polarization was performed, is usually taken as the direction of axis 3. The equation of the inverse longitudinal piezoelectric effect [7, 9] has the following form:

$$S_3 = d_{33}E_3(t) + s_{33}^E T_3(x,t), \tag{4}$$

here, $S_3 = \partial\xi(x,t)/\partial x$ is the relative displacement of the cross section of the piezoactuator, d_{33} is the piezomodule for the longitudinal piezoeffect, $E_3(t) = U(t)/\delta$ is the electric field strength, $U(t)$ is the voltage between the electrodes of actuator, δ is the thickness, s_{33}^E is the elastic compliance along axis 3, and T_3 is the mechanical stress along axis 3.

The equation of equilibrium for the forces acting on the piezoactuator (piezoelectric plate) Figure 1 can be written as

$$T_3 S_0 = F + M\frac{\partial^2\xi(x,t)}{\partial t^2} \tag{5}$$

where *F* is the external force applied to the piezoactuator, S_0 is the cross section area and *M* is the displaced mass.

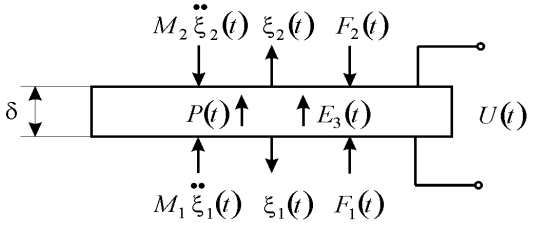

Fig. 1. Piezoactuator for the longitudinal piezoelectric effect

For constructing a structural parametric model of the voltage-controlled piezoactuator, let us solve simultaneously the wave equation, the equation of the inverse longitudinal piezoeffect, and the equation of forces acting on the faces of the piezoactuator. Calculations of the piezoactuators are performed using a wave equation [2, 7, 9] describing the wave propagation in a long line with damping but without distortions, which can be written as

$$\frac{1}{(c^E)^2}\frac{\partial^2\xi(x,t)}{\partial t^2}+\frac{2\alpha}{c^E}\frac{\partial\xi(x,t)}{\partial t}+\alpha^2\xi(x,t)=\frac{\partial^2\xi(x,t)}{\partial x^2}, \tag{6}$$

where $\xi(x,t)$ is the displacement of the section, x is the coordinate, t is time, c^E is the sound speed for $E=\text{const}$, α is the damping coefficient. Using the Laplace transform, we can reduce the original problem for the partial differential hyperbolic equation of type (6) to a simpler problem for the linear ordinary differential equation [8, 9]

Applying the Laplace transform to the wave equation (6)

$$\Xi(x,p)=L\{\xi(x,t\}=\int_0^\infty \xi(x,t)e^{-pt}dt, \tag{7}$$

setting the zero initial conditions,

$$\xi(x,t)\big|_{t=0}=0, \tag{8}$$

$$\left.\frac{\partial\xi(x,t)}{\partial t}\right|_{t=0}=0. \tag{9}$$

We obtain the linear ordinary second-order differential equation with the parameter p

$$\frac{d^2\Xi(x,p)}{dx^2}-\left[\frac{1}{(c^E)^2}p^2+\frac{2\alpha}{c^E}p+\alpha^2\right]\Xi(x,p)=0, \tag{10}$$

with its solution being the function

$$\Xi(x,p)=Ce^{-x\gamma}+Be^{x\gamma}, \tag{11}$$

where $\Xi(x,p)$ is the Laplace transform of the displacement of the section of the piezoelectric actuator, $\gamma=p/c^E+\alpha$ is the propagation coefficient. Determining coefficients C and B from the boundary conditions as

$$\Xi(0,p)=\Xi_1(p) \quad \text{for} \quad x=0, \tag{12}$$

$$\Xi(\delta,p)=\Xi_2(p) \quad \text{for} \quad x=\delta.$$

Then, the constant coefficients

$$C = \left(\Xi_1 e^{\delta\gamma} - \Xi_2\right)/\left[2\mathrm{sh}(\delta\gamma)\right], \quad B = \left(\Xi_1 e^{-\delta\gamma} - \Xi_2\right)/\left[2\mathrm{sh}(\delta\gamma)\right]. \tag{13}$$

The solution (10) can be written as

$$\Xi(x, p) = \left\{\Xi_1(p)\mathrm{sh}\left[(\delta - x)\gamma\right] + \Xi_2(p)\mathrm{sh}(x\gamma)\right\}/\mathrm{sh}(\delta\gamma). \tag{14}$$

The equations for the forces on the faces of the piezoactuator

$$T_3(0, p)S_0 = F_1(p) + M_1 p^2 \Xi_1(p) \quad \text{for} \quad x = 0, \tag{15}$$

$$T_3(\delta, p)S_0 = -F_2(p) + M_2 p^2 \Xi_1(p) \quad \text{for} \quad x = \delta,$$

where $T_3(0, p)$ and $T_3(\delta, p)$ are determined from the equation of the inverse piezoelectric effect.

For $x = 0$ and $x = \delta$, we obtain the following set of equations for determining stresses in the piezoactuator [24 − 26]:

$$T_3(0, p) = \frac{1}{s_{33}^E}\frac{d\Xi(x, p)}{dx}\bigg|_{x=0} - \frac{d_{33}}{s_{33}^E}E_3(p), \tag{16}$$

$$T_3(\delta, p) = \frac{1}{s_{33}^E}\frac{d\Xi(x, p)}{dx}\bigg|_{x=\delta} - \frac{d_{33}}{s_{33}^E}E_3(p).$$

The set of equations (16) yield the set of equations for the structural-parametric model of the piezoactuator Figure 2:

$$\begin{aligned}
\Xi_1(p) &= \left[1/\left(M_1 p^2\right)\right]\left\{-F_1(p) + \left(1/\chi_{33}^E\right)\left[d_{33}E_3(p) - \left[\gamma/\mathrm{sh}\left(\delta\gamma\right)\right]\left[\mathrm{ch}\left(\delta\gamma\right)\Xi_1(p) - \Xi_2(p)\right]\right]\right\} \\
\Xi_2(p) &= \left[1/\left(M_2 p^2\right)\right]\left\{-F_2(p) + \left(1/\chi_{33}^E\right)\left[d_{33}E_3(p) - \left[\gamma/\mathrm{sh}\left(\delta\gamma\right)\right]\left[\mathrm{ch}\left(\delta\gamma\right)\Xi_2(p) - \Xi_1(p)\right]\right]\right\}
\end{aligned} \tag{17}$$

where $\chi_{33}^E = s_{33}^E/S_0$.

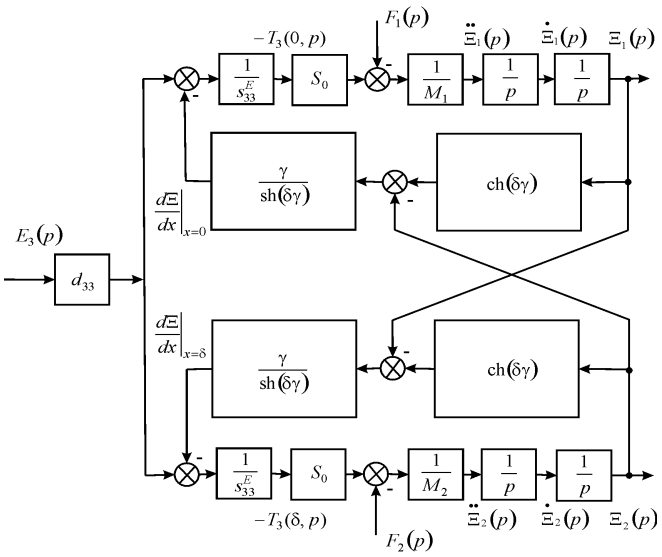

Fig. 2. Parametric structural schematic diagram of a voltage-controlled piezoactuator for longitudinal piezoelectric effect

The equation of the inverse transverse piezoeffect [7, 9]

$$S_1 = d_{31}E_3(t) + s_{11}^E T_1(x,t) \ , \tag{18}$$

where $S_1 = \partial\xi(x,t)/\partial x$ is the relative displacement of the cross section along axis 1 Figure 3, d_{31} is the piezoelectric module for the transverse piezoeffect, s_{11}^E is the elastic compliance along axis 1, T_1 is the stress along axis 1.

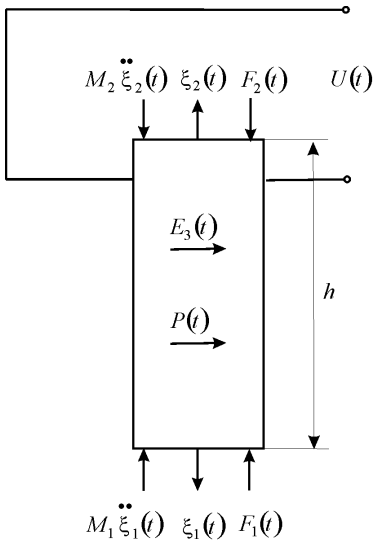

Fig. 3. Piezoactuator for the transverse piezoelectric effect

The solution of the linear ordinary differential equation (10) can be written as (11), where the constants C and B in the form

$$\Xi(0, p) = \Xi_1(p) \quad \text{for} \quad x = 0\,, \tag{19}$$

$$\Xi(l, p) = \Xi_2(p) \quad \text{for} \quad x = h\,,$$

$$C = \left(\Xi_1 e^{h\gamma} - \Xi_2\right) / \left[2\mathrm{sh}(h\gamma)\right]\,, \quad B = \left(\Xi_1 e^{-h\gamma} - \Xi_2\right) / \left[2\mathrm{sh}(h\gamma)\right]\,. \tag{20}$$

Then, the solution (10) can be written as

$$\Xi(x, p) = \left\{\Xi_1(p)\mathrm{sh}\left[(h - x)\gamma\right] + \Xi_2(p)\mathrm{sh}(x\gamma)\right\} / \mathrm{sh}(h\gamma)\,. \tag{21}$$

The equations of forces acting on the faces of the piezoactuator

$$T_1(0, p)S_0 = F_1(p) + M_1 p^2 \Xi_1(p) \quad \text{for} \quad x = 0, \tag{22}$$

$$T_1(h, p)S_0 = -F_2(p) + M_2 p^2 \Xi_2(p) \quad \text{for} \quad x = h,$$

where $T_1(0, p)$ and $T_1(h, p)$ are determined from the equation of the inverse piezoeffect [24 − 26]. Thus, we obtain

$$\begin{aligned} T_1(0, p) &= \frac{1}{s_{11}^E} \left.\frac{d\Xi(x, p)}{dx}\right|_{x=0} - \frac{d_{31}}{s_{11}^E} E_3(p), \\ T_1(h, p) &= \frac{1}{s_{11}^E} \left.\frac{d\Xi(x, p)}{dx}\right|_{x=h} - \frac{d_{31}}{s_{11}^E} E_3(p). \end{aligned} \tag{23}$$

The set of equations (23) for mechanical stresses in piezoactuator yields the following set of equations describing the structural-parametric model and parametric structural schematic diagram of piezoactuator Figure 4

$$\begin{aligned} \Xi_1(p) &= \left[1/\left(M_1 p^2\right)\right]\left\{-F_1(p) + \left(1/\chi_{11}^E\right)\left[d_{31}E_3(p) - \left[\gamma/\mathrm{sh}\left(h\gamma\right)\right]\left[\mathrm{ch}\left(h\gamma\right)\Xi_1(p) - \Xi_1(p)\right]\right]\right\}, \\ \Xi_2(p) &= \left[1/\left(M_2 p^2\right)\right]\left\{-F_2(p) + \left(1/\chi_{11}^E\right)\left[d_{31}E_3(p) - \left[\gamma/\mathrm{sh}\left(h\gamma\right)\right]\left[\mathrm{ch}\left(h\gamma\right)\Xi_2(p) - \Xi_1(p)\right]\right]\right\}, \end{aligned} \tag{24}$$

where $\chi_{11}^E = s_{11}^E / S_0$.

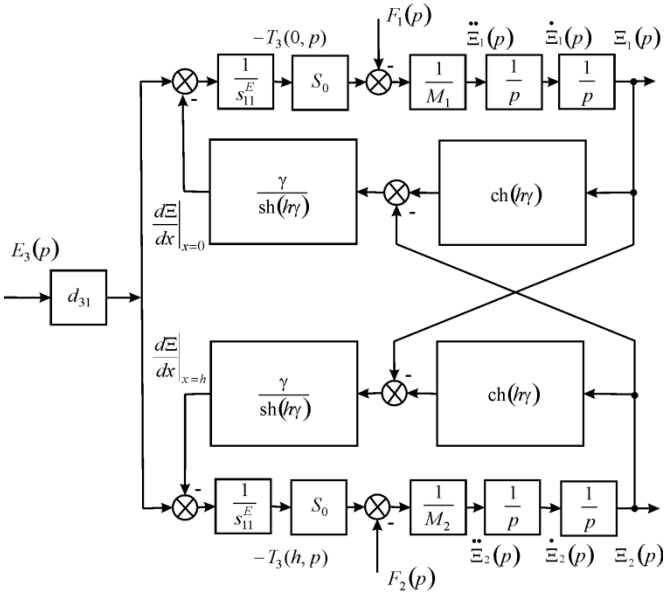

Fig. 4. Parametric structural schematic diagram of a voltage-controlled piezoactuator for transverse piezoelectric effect

Let us consider the piezoactuator for the shift piezoelectric effect Figure 5.

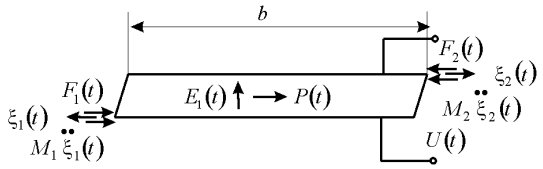

Fig. 5. Piezoactuator for the shift piezoelectric effect

We obtain the following set of equations describing the structural-parametric model and parametric structural schematic diagram of piezoactuator Figure 6

$$\Xi_1(p) = \left[1/\left(M_1 p^2\right)\right]\left\{-F_1(p) + \left(1/\chi_{55}^E\right)\left[d_{15}E_1(p) - \left[\gamma/\mathrm{sh}\left(b\gamma\right)\right]\left[\mathrm{ch}\left(b\gamma\right)\Xi_1(p) - \Xi_1(p)\right]\right]\right\}, \tag{25}$$

$$\Xi_2(p) = \left[1/\left(M_2 p^2\right)\right]\left\{-F_2(p) + \left(1/\chi_{55}^E\right)\left[d_{15}E_1(p) - \left[\gamma/\mathrm{sh}\left(b\gamma\right)\right]\left[\mathrm{ch}\left(b\gamma\right)\Xi_2(p) - \Xi_1(p)\right]\right]\right\},$$

where $\chi_{55}^E = s_{55}^E/S_0$.

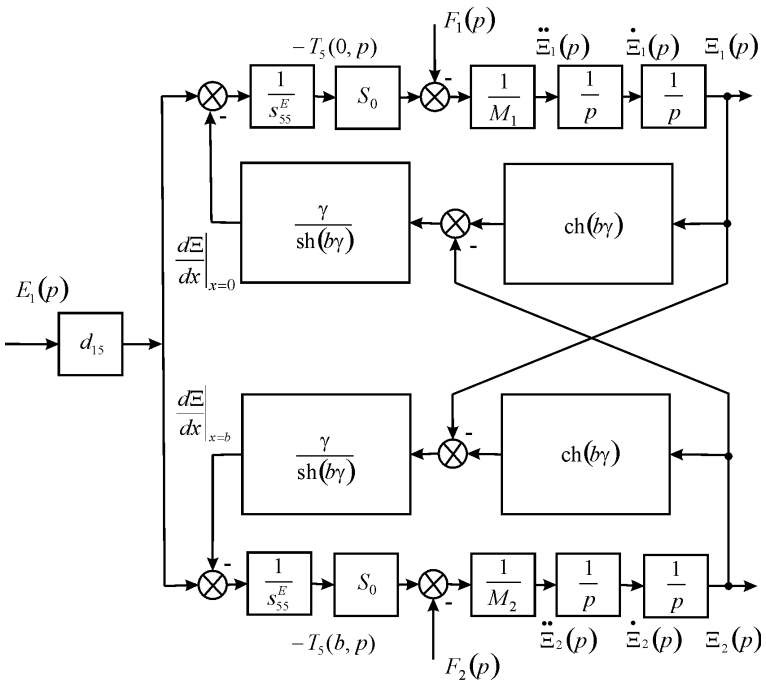

Fig. 6. Parametric structural schematic diagram of a voltage-controlled piezoactuator for shift piezoelectric effect

From (17), (24), (25) we obtain the system of equations describing the generalized structural-parametric model of actuator

$$\Xi_1(p) = \left[1/\left(M_1 p^2\right)\right]\left\{ -F_1(p) + \left(1/\chi_{ij}^{\Psi}\right)\left[\nu_{mi}\Psi_m(p) - \left[\gamma/\mathrm{sh}(l\gamma)\right]\left[\mathrm{ch}(l\gamma)\Xi_1(p) - \Xi_2(p)\right]\right]\right\}, \tag{26}$$

$$\Xi_2(p) = \left[1/\left(M_2 p^2\right)\right]\left\{ -F_2(p) + \left(1/\chi_{ij}^{\Psi}\right)\left[\nu_{mi}\Psi_m(p) - \left[\gamma/\mathrm{sh}(l\gamma)\right]\left[\mathrm{ch}(l\gamma)\Xi_2(p) - \Xi_1(p)\right]\right]\right\},$$

where $\nu_{mi} = \begin{cases} d_{33}, d_{31}, d_{15} \\ g_{33}, g_{31}, g_{15} \\ d_{33}, d_{31}, d_{15} \end{cases}$, $\Psi_m = \begin{cases} E_3, E_1 \\ D_3, D_1 \\ H_3, H_1 \end{cases}$, $s_{ij}^{\Psi} = \begin{cases} s_{33}^E, s_{11}^E, s_{55}^E \\ s_{33}^D, s_{11}^D, s_{55}^D \\ s_{33}^H, s_{11}^H, s_{55}^H \end{cases}$, $c^{\Psi} = \begin{cases} c^E \\ c^D \\ c^H \end{cases}$, $\gamma = \begin{cases} \gamma^E \\ \gamma^D \\ \gamma^H \end{cases}$, $l = \begin{cases} \delta \\ h \\ b \end{cases}$, $\chi_{ij}^{\Psi} = s_{ij}^{\Psi} / S_0$,

then parameters Ψ of the control for the electromagnetoelastic actuator: *E* for voltage control, *D* for current control, *H* for magnetic field strength control. Figure 7 shows the generalized parametric structural schematic diagram of the electromagnetoelastic actuator corresponding to the set of equations (26).

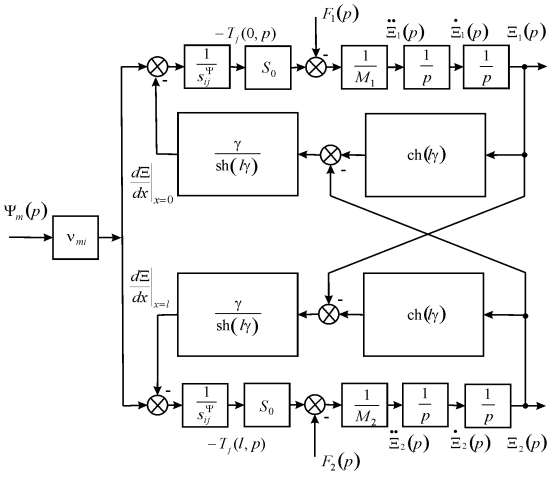

Fig. 7. Generalized parametric structural schematic diagram of the electromagnetoelastic actuator

3. Transfer Functions of Electromagnetoelastic Actuator

Generalized structural-parametric model (26) of the actuator after algebraic transformations provides the transfer functions of the actuator in matrix form [24-26], where the transfer functions are the ratio of the Laplace transform of the displacement of the face and the Laplace transform of the corresponding parameter or force at zero initial conditions.

$$\Xi_1(p) = W_{11}(p)\Psi_m(p) + W_{12}(p)F_1(p) + W_{13}(p)F_2(p), \tag{27}$$

$$\Xi_2(p) = W_{21}(p)\Psi_m(p) + W_{22}(p)F_1(p) + W_{23}(p)F_2(p),$$

where the generalized transfer functions of the electromagnetoelastic actuator are

$$W_{11}(p) = \Xi_1(p)/\Psi_m(p) = \nu_{mi}\left[M_2\chi_{ij}^{\Psi}p^2 + \gamma\mathrm{th}(l\gamma/2)\right]/A_{ij},$$

$$A_{ij} = M_1M_2\left(\chi_{ij}^{\Psi}\right)^2 p^4 + \left\{(M_1+M_2)\chi_{ij}^{\Psi}/\left[c^{\Psi}\mathrm{th}(l\gamma)\right]\right\}p^3 + \left[(M_1+M_2)\chi_{ij}^{\Psi}\alpha/\mathrm{th}(l\gamma) + 1/\left(c^{\Psi}\right)^2\right]p^2 + 2\alpha p/c^{\Psi} + \alpha^2,$$

$$W_{21}(p) = \Xi_2(p)/\Psi_m(p) = \nu_{mi}\left[M_1\chi_{ij}^{\Psi}p^2 + \gamma\mathrm{th}(l\gamma/2)\right]/A_{ij},$$

$$W_{12}(p) = \Xi_1(p)/F_1(p) = -\chi_{ij}^{\Psi}\left[M_2\chi_{ij}^{\Psi}p^2 + \gamma/\mathrm{th}(l\gamma)\right]/A_{ij},$$

$$W_{13}(p) = \Xi_1(p)/F_2(p) = W_{22}(p) = \Xi_2(p)/F_1(p) = \left[\chi_{ij}^{\Psi}\gamma/\mathrm{sh}(l\gamma)\right]/A_{ij},$$

$$W_{23}(p) = \Xi_2(p)/F_2(p) = -\chi_{ij}^{\Psi}\left[M_1\chi_{ij}^{\Psi}p^2 + \gamma/\mathrm{th}(l\gamma)\right]/A_{ij}.$$

Therefore, we obtain from equations (27) the generalized matrix equaion for the electromagnetoelastic

actuator

$$\begin{pmatrix} \Xi_1(p) \\ \Xi_2(p) \end{pmatrix} = \begin{pmatrix} W_{11}(p) & W_{12}(p) & W_{13}(p) \\ W_{21}(p) & W_{22}(p) & W_{23}(p) \end{pmatrix} \begin{pmatrix} \Psi_m(p) \\ F_1(p) \\ F_2(p) \end{pmatrix}. \tag{28}$$

Let us find the displacement of the faces the electromagnetoelastic actuator in a stationary regime for $\Psi_m(t) = \Psi_{m0} \cdot 1(t)$, $F_1(t) = F_2(t) = 0$ and inertial load. The static displacement of the faces the electromagnetoelastic actuator $\xi_1(\infty)$ and $\xi_2(\infty)$ can be written in the form:

$$\xi_1(\infty) = \lim_{t\to\infty} \xi_1(t) = \lim_{\substack{p\to 0 \\ \alpha\to 0}} pW_{11}(p)\Psi_{m0}/p = \nu_{mi} l \Psi_{m0} (M_2 + m/2)/(M_1 + M_2 + m), \tag{29}$$

$$\xi_2(\infty) = \lim_{t\to\infty} \xi_2(t) = \lim_{\substack{p\to 0 \\ \alpha\to 0}} pW_{21}(p)\Psi_{m0}/p = \nu_{mi} l \Psi_{m0} (M_1 + m/2)/(M_1 + M_2 + m), \tag{30}$$

$$\xi_1(\infty) + \xi_2(\infty) = \lim_{t\to\infty}(\xi_1(t) + \xi_2(t)) = \nu_{mi} l \Psi_{m0}, \tag{31}$$

where m is the mass of the electromagnetoelastic actuator, M_1, M_2 are the load masses.

Let us consider a numerical example of the calculation of static characteristics of the piezoactuator from piezoceramics PZT under the longitudinal piezoelectric effect at $m << M_1$ and $m << M_2$. For $d_{33} = 4 \cdot 10^{-10}$ m/V, $U = 125$ V, $M_1 = 10$ kg and $M_2 = 40$ kg we obtain the static displacement of the faces of the piezoactuator $\xi_1(\infty) = 40$ nm, $\xi_2(\infty) = 10$ nm, $\xi_1(\infty) + \xi_2(\infty) = 50$ nm.

The static displacement the faces of the piezoactuator for the transverse piezoelectric effect and inertial load at $U(t) = U_0 \cdot 1(t)$, $E_3(t) = E_{30} \cdot 1(t) = (U_0/\delta) \cdot 1(t)$ and $F_1(t) = F_2(t) = 0$ can be written in the following form:

$$\xi_1(\infty) = \lim_{t\to\infty} \xi_1(t) = \lim_{\substack{p\to 0 \\ \alpha\to 0}} pW_{11}(p)(U_0/\delta)/p = d_{31}(h/\delta) U_0 (M_2 + m/2)/(M_1 + M_2 + m), \tag{32}$$

$$\xi_2(\infty) = \lim_{t\to\infty} \xi_2(t) = \lim_{\substack{p\to 0 \\ \alpha\to 0}} pW_{21}(p)(U_0/\delta)/p = d_{31}(h/\delta) U_0 (M_1 + m/2)/(M_1 + M_2 + m), \tag{33}$$

$$\xi_1(\infty) + \xi_2(\infty) = \lim_{t\to\infty}(\xi_1(t) + \xi_2(t)) = d_{31}(h/\delta) U_0. \tag{34}$$

The static displacement of the faces of the piezoactuator for the transverse piezoelectric effect at $m << M_1$ and $m << M_2$

$$\xi_1(\infty)=\lim_{t\to\infty}\xi_1(t)=\lim_{\substack{p\to 0\\ \alpha\to 0}} pW_{11}(p)(U_0/\delta)/p = d_{31}(h/\delta)U_0 M_2/(M_1+M_2), \tag{35}$$

$$\xi_2(\infty)=\lim_{t\to\infty}\xi_2(t)=\lim_{\substack{p\to 0\\ \alpha\to 0}} pW_{21}(p)(U_0/\delta)/p = d_{31}(h/\delta)U_0 M_1/(M_1+M_2). \tag{36}$$

Let us consider a numerical example of the calculation of static characteristics of the piezoactuator from piezoceramics PZT under the transverse piezoelectric effect at $m << M_1$ and $m << M_2$. For $d_{31}=2.5\cdot 10^{-10}$ m/V, $h=4\cdot 10^{-2}$ m, $\delta=2\cdot 10^{-3}$ m, $U=100$ V, $M_1=10$ kg and $M_2=40$ kg we obtain the static displacement of the faces of the piezoelectric actuator $\xi_1(\infty)=400$ nm, $\xi_2(\infty)=100$ nm, $\xi_1(\infty)+\xi_2(\infty)=500$ nm.

For the description of the piezoactuator for the longitudinal piezoelectric effect for one rigidly fixed face of the transducer at $M_1\to\infty$ we obtain from equation (28) the transfer functions $W_{21}(p)$ and $W_{23}(p)$ of the piezoactuator for the longitudinal piezoelectric effect in the following form:

$$W_{21}(p)=\Xi_2(p)/E_3(p)=d_{33}\delta/\left[M_2\delta\chi_{33}^E p^2+\delta\gamma\,\mathrm{cth}(\delta\gamma)\right], \tag{37}$$

$$W_{23}(p)=\Xi_2(p)/F_2(p)=-\delta\chi_{33}^E/\left[M_2\delta\chi_{33}^E p^2+\delta\gamma\,\mathrm{cth}(\delta\gamma)\right]. \tag{38}$$

Accordingly, the static displacement $\xi_2(\infty)$ of the piezoactuator under the longitudinal piezoeffect in the form

$$\xi_2(\infty)=\lim_{t\to\infty}\xi_2(t)=\lim_{p\to 0} pW_2(p)U_0/p = d_{33}U_0, \tag{39}$$

$$\xi_2(\infty)=\lim_{p\to 0} pW_{23}(p)F_0/p = -\delta s_{33}^E F_0/S_0. \tag{40}$$

Let us consider a numerical example of the calculation of static characteristics of the piezoactuator under the longitudinal piezoeffects. For $d_{33}=5\cdot 10^{-10}$ m/V, $U=250$ V we obtain $\xi_2(\infty)=125$ nm. For $\delta=6\cdot 10^{-4}$ m, $s_{33}^E=3.5\cdot 10^{-11}$ m^2/N, $F_0=1000$ N, $S_0=1.75\cdot 10^{-4}$ m^2 we obtain $\xi_2(\infty)=-120$ nm. The experimental and calculated values for the piezoactuator are in agreement to an accuracy of 5%.

Let us consider the operation at low frequencies for the piezoactuator with one face rigidly fixed so that $M_1\to\infty$ and $m << M_2$. Using the approximation of the hyperbolic cotangent by two terms of the power series in transfer functions (37) and (38), at $m << M_2$ we obtain the expressions in the frequency range of $0<\omega<0{,}01c^E/\delta$

$$W_{21}(p)=\Xi_2(p)/E_3(p)=d_{33}\delta/\left(T_t^2 p^2+2T_t\xi_t p+1\right), \tag{41}$$

$$W_{23}(p) = \Xi_2(p)/F_2(p) = -\left(s_{33}^E \delta / S_0\right)/\left(T_t^2 p^2 + 2T_t \xi_t p + 1\right), \tag{42}$$

$$T_t = \left(\delta / c^E\right)\sqrt{M_2/m} = \sqrt{M_2/C_{33}^E}\ ,\ \ \xi_t = (\alpha\delta/3)\sqrt{m/M_2}\ ,\ \ C_{33}^E = S_0/\left(s_{33}^E\delta\right) = 1/\left(\chi_{33}^E\delta\right).$$

where T_t is the time constant and ξ_t is the damping coefficient, C_{33}^E - is the is rigidity of the piezoactuator under the longitudinal piezoeffect.

In the static mode of operation the piezoactuator for elastic load we obtain the equation the following form

$$\frac{\xi_2}{\xi_{2m}} = \frac{1}{1 + C_e/C_{33}^E}, \tag{43}$$

where ξ_2 is the displacement of the piezoactuator in the case of the elastic load, $\xi_{2m} = d_{33}U_0$ is the maximum displacement of the piezoactuator, C_e is the load rigidity.

From (41), (43) we obtain the transfer functions of the piezoactuator with a fixed end and elastic inertial load

$$W_2(p) = \frac{\Xi_2(p)}{U(p)} = \frac{d_{33}}{\left(1 + C_e/C_{33}^E\right)\left(T_t^2 p^2 + 2T_t\xi_t p + 1\right)} \tag{44}$$

where the time constant T_t and the damping coefficient ξ_t are determined by the formulas

$$T_t = \sqrt{M_2/\left(C_e + C_{33}^E\right)},\ \ \xi_t = \alpha\delta^2 C_{33}^E \Big/ \left(3c^E\sqrt{M\left(C_e + C_{33}^E\right)}\right).$$

Let us consider the operation at low frequencies for the piezoactuator with one face rigidly fixed and elastic inertial load so that $M_1 \to \infty$ and $m << M_2$ for $M_2 = 10\,\text{kg}, C_{33} = 2.3\cdot 10^6\,\text{N/m}$, $C_e = 0.2\cdot 10^6\,\text{N/m}$ we obtain $T_t = 2\cdot 10^{-3}\,\text{c}$.

4. Results and Discussions

We obtain a generalized parametric structural schematic diagram of electromagnetoelastic actuator for nano- and micromanipulators of biological and chemical research Figure 7 taking into account equation of generalized electromagnetoelasticity (piezoelectric, piezomagnetic, electrostriction, and magnetostriction effects) and decision wave equation. The results of constructing a generalized structural-parametric model and a generalized parametric structural schematic diagram of electromagnetoelastic actuator for the longitudinal, transverse and shift deformations are shown in Figure 7. Parametric structural schematic diagrams piezoelectric actuator for longitudinal, transverse, shift piezoelectric effects Figure 2, Figure 4, Figure 6 converts to generalized parametric structural schematic diagram of the electromagnetoelastic actuator Figure

7 with the replacement of the following parameters

$$\Psi_m = E_3, E_3, E_1, \quad \nu_{mi} = d_{33}, d_{31}, d_{15}, \quad s_{ij}^{\Psi} = s_{33}^{E}, s_{11}^{E}, s_{55}^{E}, \quad l = \delta, h, b.$$

Generalized structural-parametric model and generalized parametric structural schematic diagram of the electromagnetoelastic actuator after algebraic transformations provides the transfer functions of the electromagnetoelastic actuator actuator for nano- and micromanipulators of biological and chemical research. The piezoelectric actuator with the transverse piezoelectric effect compared to the piezoelectric actuator for the longitudinal piezoelectric effect provides a greater range of static displacement and a less working force. The magnetostriction actuators provides a greater range of static working forces.

It is possible to construct the generalized structural-parametric model, generalized parametric structural schematic diagram and the transfer functions in matrix form of the electromagnetoelastic actuator using the solutions of the wave equation of the electromagnetoelastic actuator and taking into account the features of the deformations actuator along the coordinate axes.

5. Conclusions

Using the obtained solutions of the wave equation and taking into account the features of the deformations along the coordinate axes, it is possible to construct the generalized structural-parametric model and parametric structural schematic diagram of the electromagnetoelastic actuator for nano- and micromanipulators of biological and chemical research and to describe its dynamic and static properties.

The transfer functions and the parametric structural schematic diagram of the piezoactuators for the transverse, longitudinal, shift piezoelectric effects are obtained from structural-parametric models of the piezoactuators.

The transfer functions in matrix form of the electromagnetoelastic are describe deformations actuator during its operation as a part of the control systems for nano- and micromanipulators of biological and chemical research.

References

[1] Uchino, K. (1997) Piezoelectric actuator and ultrasonic motors. Boston, MA: Kluwer Academic Publisher, 347 p.

[2] Afonin, S.M. (2006) Solution of the wave equation for the control of an elecromagnetoelastic transduser. *Doklady mathematics*, 73, 2, 307-313, doi:10.1134/S1064562406020402.

[3] Afonin, S.M. (2008) Structural parametric model of a piezoelectric nanodisplacement transduser. *Doklady physics*,

53, 3, 137-143, doi:10.1134/S1028335808030063.

[4] Afonin, S.M. (2014) Stability of strain control systems of nano-and microdisplacement piezotransducers. *Mechanics of solids*, 49, 2, 196-207, doi:10.3103/S0025654414020095.

[5] Yang, Y. , Tang, L. (2009) Equivalent circuit modeling of piezoelectric energy harvesters, *Journal of intelligent material systems and structures*, 20, 18, 2223-2235.

[6] Cady, W.G. (1946) Piezoelectricity an introduction to the theory and applications of electromechancial phenomena in crystals. New York, London: McGraw-Hill Book Company, 806 p.

[7] Physical Acoustics: Principles and Methods. (1964) Vol.1. Part A. Methods and Devices. Ed.: W. Mason. New York: Academic Press. 515 p.

[8] Zwillinger, D. (1989) Handbook of Differential Equations. Boston: Academic Press. 673 p.

[9] Afonin, S.M. (2015) Structural-parametric model and transfer functions of electroelastic actuator for nano- and microdisplacement, Chapter 9 in *Piezoelectrics and Nanomaterials: Fundamentals, Developments and Applications*. Ed. I.A. Parinov. New York: Nova Science. pp. 225-242.

[10] Afonin, S.M. (2005) Generalized parametric structural model of a compound elecromagnetoelastic transduser. *Doklady physics*, 50, 2, 77-82, doi:10.1134/1.1881716.

[11] Afonin, S.M. (2002) Parametric structural diagram of a piezoelectric converter. *Mechanics of solids*, 37, 6, 85-91.

[12] Afonin, S.M. (2003) Deformation, fracture, and mechanical characteristics of a compound piezoelectric transducer. *Mechanics of solids*, 38, 6, 78-82.

[13] Afonin, S.M. (2004) Parametric block diagram and transfer functions of a composite piezoelectric transducer. *Mechanics of solids*, 39, 4, 119-127.

[14] Afonin, S.M. (2007) Elastic compliances and mechanical and adjusting characteristics of composite piezoelectric transducers. *Mechanics of solids*, 42, 1, 43-49, doi:10.3103/S0025654407010062.

[15] Afonin, S.M. (2009) Static and dynamic characteristics of a multy-layer electroelastic solid. *Mechanics of solids*, 44, 6, 935-950, doi:10.3103/S0025654409060119.

[16] Afonin, S.M. (2010) Design static and dynamic characteristics of a piezoelectric nanomicrotransducers. *Mechanics of solids*, 45, 1, 123-132, doi:10.3103/S0025654410010152.

[17] Afonin, S.M. (2001) Structural-parametric model of nanometer-resolution piezomotor. *Russian engineering research*, 21, 5, 42-50.

[18] Afonin, S.M. (2002) Parametric structure of composite nanometric piezomotor. *Russian engineering research*, 22, 12, 9-24.

[19] Afonin, S.M. (2011) Electromechanical deformation and transformation of the energy of a nano-scale piezomotor. *Russian engineering research*, 31, 7, 638-642, doi:10.3103/S1068798X11070033.

[20] Afonin, S.M. (2011) Electroelasticity problems for multilayer nano- and micromotors. *Russian engineering research*, 31, 9, 842-847, doi:10.3103/S1068798X11090036.

[21] Afonin, S.M. (2012) Nano- and micro-scale piezomotors. *Russian engineering research*, 32, 7-8, 519-522, doi:10.3103/S1068798X12060032.

[22] Afonin, S.M. (2015) Dynamic characteristics of multilayer piezoelectric nano- and micromotors. *Russian engineering research*, 35, 2, 89-93, doi:10.3103/S1068798X15020045.

[23] Afonin, S.M. (2015) Optimal control of a multilayer submicromanipulator with a longitudinal piezo effect. *Russian engineering research*, 35, 12, 907-910, doi:10.3103/S1068798X15120035.

[24] Afonin, S.M. (2005) Generalized structural parametric model of an elecromagnetoelastic transduser for control system of nano- and microdisplacement: I. Solution of the wave equation for control problem of an elecromagnetoelastic transduser. *Journal of computer and systems sciences international*, 44, 3, 399-405.

[25] Afonin, S.M. (2005) Generalized structural parametric model of an elecromagnetoelastic transduser for control system of nano- and microdisplacements: II. On the generalized structural parametric model of a compound elecromagnetoelastic transduser. *Journal of computer and systems sciences international*, 44, 4, 606-612.

[26] Afonin, S.M. (2006) Generalized structural-parametric model of an elecromagnetoelastic converter for nano- and micrometric movement control systems: III. Transformation parametric structural circuits of an elecromagnetoelastic converter for nano- and micromovement control systems. *Journal of computer and systems sciences international*, 45, 2, 317-325, doi:10.1134/S106423070602016X.

[27] Afonin, S.M. (2015) Block diagrams of a multilayer piezoelectric motor for nano- and microdisplacements based on the transverse piezoeffect. *Journal of computer and systems sciences international*, 54, 3, 424-439, doi:10.1134/S1064230715020021.

[28] Afonin, S.M. (2006) Absolute stability conditions for a system controlling the deformation of an elecromagnetoelastic transduser. *Doklady mathematics*, 74, 3, 943-948, doi:10.1134/S1064562406060391.

[29] Springer Handbook of Nanotechnology. (2004) Ed. by B. Bhushan. Berlin, New York: Springer, 1222 p

[30] Encyclopedia of Nanoscience and Nanotechnology. (2004) Ed. by H. S. Nalwa. Calif.: American Scientific Publishers.